



IDENTIFICATION OF INTERFACIAL STRESS PATTERN ON DENTIN POST SURFACE

*Identificação do padrão de estresse na interface entre
as superfícies da dentina e do pino*

Muhammet Vefa Akpinar^a, Yusuf Ziya Akpinar^b

^a PhD, Department of Civil Engineering, Karadeniz Technical University, Trabzon, Turkey, e-mail: mvakpinar@yahoo.com

^b DDS, PhD, Vezir Kopru Devlet Hastahanesi, Vezirkopru, Samsun, Turkey.

Abstract

OBJECTIVE: The purpose of this study was to develop an interfacial stress distribution model for the post -dentin interface due to 50, 100 and 250 Newton occlusal biting forces by utilizing a finite element model. The hypothesis of the present study is that, on the basis of these interfacial stress models for post-dentine, it is possible to compute interfacial stresses at any given point on the post dentin surface and capture the characteristic behavior of post under the specific loading conditions under consideration. **MATERIAL AND METHOD:** The two-dimensional FEM was created by a self-developed image processing system, manually digitizing the key points on dental cross-section boundaries obtained from an actual maxillary canine tooth image. Crown, post core and coronal-radicular restoration were modeled by creating key points and transferring them to a two-dimensional coordinate XY system in the FE environment. The generated post in the model was 1.4 mm in diameter and 15 mm in length. A finite element (FE) analysis was performed to investigate the interfacial shear stress distribution on the dentine-post interface frequently used for the restoration of endodontically treated teeth. **RESULTS AND CONCLUSION:** From the results and within the limitations of the present study it can be concluded that the interfacial stress along the post is nonlinear and is roughly sinusoidal and the peak interfacial stress between the post and the dentin is expected to occur on top of the post. Sinusoidal models were developed to generalize the interfacial stress nonlinearity along the post length. These models can be used for calculation of the interfacial shear stress for 50, 100, and 250 Newton forces applied compressively at 45 degrees angle with respect to the implant axis. This study showed that the interfacial stress along the post was nonlinear and appeared roughly sinusoidal. Regression models were developed to generalize the interfacial stress nonlinearity along the post length.

Keywords: Interfacial shear stress. Pattern post. FEM. Dental materials.

Resumo

OBJETIVO: O objetivo deste estudo foi desenvolver um modelo de distribuição do estresse interfacial para a interface pino-dentina devido a forças oclusais (mordida) geradas por 50, 100 e 250 Newton, utilizando um modelo de elementos finitos. A hipótese do presente estudo é que, baseado neste modelo de estresse interfacial (dentina-pino), é possível computar estresses interfaciais em qualquer ponto determinado na interface pino-dentina e capturar o comportamento característico do pino submetido a condições de carga diversas. **MATERIAL E MÉTODO:** o FEM bidimensional foi criado por um sistema de processamento de imagem autodesenvolvido, digitando-se manualmente os pontos-chave nos limites das seções obtidos de uma imagem real de dente canino. A coroa, o pino e a restauração radicular coronal foram moldados criando pontos-chave e transferindo-os para uma coordenada bi-dimensional (sistema XY) no ambiente FE. O pino gerado no modelo foi de 1.4 mm de diâmetro e 15 mm de comprimento. Uma análise de elementos finitos foi efetuada para investigar a distribuição do estresse de deslizamento na interface dentina-pino, usada com frequência para a restauração de dentes tratados endodonticamente. **RESULTADOS E CONCLUSÃO:** Pelos resultados e com as limitações do presente estudo, pode ser concluído que o estresse interfacial entre o pino e a dentina é não linear, grosseiramente sinusoidal e o pico de estresse interfacial entre pino e dentina é de ocorrência esperada no topo do pino. Modelos sinusoidais foram desenvolvidos para generalizar o estresse interfacial não linearmente ao longo do comprimento do pino. Estes modelos podem ser usados para cálculo da força de cisalhamento frente a forças de 50, 100, 250 N aplicadas compressivamente em ângulo de 45 graus em relação ao eixo do implante. Este estudo demonstrou que o estresse interfacial ao longo do pino foi não linear, sendo grosseiramente sinusoidal. Modelos de regressão foram desenvolvidos para generalizar o estresse interfacial não linearmente ao longo do comprimento do pino.

Palavras-chave: Estresse em forças de cisalhamento. Materiais dentários. Padrão de pino. FEM.

INTRODUCTION

The interfacial strength between dental materials is an important criterion to predict clinical behavior. In a tooth system made with many components that differ in mechanical properties, the interface between the components represents the critical area of the system itself.

Determination of the stress distributions in post-core restored endodontically treated teeth is challenging due to the fact that the post and core systems have small dimensions and are structurally complex. To understand the mechanisms responsible of tooth failure, the stress distribution within restored and unrestored teeth that results from mastication force has been studied extensively. Several studies have used finite element techniques in attempts to gain understanding of the process of stress dissipation in teeth.

The FEM is a valid technique for analyzing the mechanical behavior of complex structures.

Available finite element programs are powerful tools for studying stress-strain analysis in tooth structures, and have been used in early dental studies as an analytical tool in biomechanical research.

Several studies have identified the nonuniform stress distributions along post-dentin bonded interfaces. Holmes et al. (1) predicted the distribution of stresses in dentin of an endodontically treated tooth restored with cast post and cores by using FE analyses. They found that the distribution of tensile and compressive stresses was not affected with variation in the dimensions of the posts. Peak dentinal shear stresses occurred adjacent to the post at mid-root. Peak shear stresses were elevated as the length of the post decreased. Peak dentinal tensile stresses occurred in the gingival third of the facial root surface, whereas peak dentinal compressive stresses were evident in the gingival third of the lingual root surface.

De Santis et al. (2) evaluated the mechanical resistance of posts cemented in human

dentine by the means of mechanical pullout tests assisted by the finite element analysis. The average bond strength and the critical stress values of the post-cement interface were 25 MPa and 50 MPa respectively. Burns et al (3) compared the stress distribution during insertion and function of three prefabricated endodontic posts. Specimens were subjected to 135 N oblique force applied at 26 degrees. Para-Post posts showed evenly distributed patterns of stress and Flexi-Post posts formed asymmetric stress patterns with concentration of stress at each thread. A comparative study by Alessandro et al. (4) on the stress distribution in the dentine and cement layer of an endodontically treated maxillary incisor was carried out by using Finite Element Analysis (FEA). A chewing static force of 10 N was applied at 125 angle with the tooth longitudinal axis at the palatal surface of the crown. The differences in occlusal load transfer ability when carbon, steel, and glass posts, fixed to root canal using luting cements of different elastic moduli (7.0 and 18.7 GPa) were discussed. Maximum Von Mises equivalent stress values ranging from 7.5 (steel) to 5.4 and 3.6 MPa (respectively, for carbon posts fixed with high and low cement moduli) and to 2.2 MPa (either for glass posts fixed with high and low cement moduli) were observed. Their study concluded that a very stiff post works against the natural function of the tooth creating zones of tension and shear both in the dentine and at the interfaces of the luting cement and the post.

Hypothesis

A variety of 2-D and 3-D FE analysis have been described to determine the peak stresses on the bond strength of post to dentine. Unfortunately, these studies have not defined the generalized behavior of the interfacial stress distribution. Modeling of the response of post dentin interfaces is necessary to obtain adequate estimates of interfacial stress magnitudes. The hypothesis of the present study is that, on the basis of these interfacial stress models for post-dentine, it is possible to compute interfacial stresses at any given point on the post dentin surface and capture the characteristic behavior of post under the specific loading conditions under consideration.

MATERIALS AND METHODS

The interfacial stress distribution between the dentin and the post of an endodontically treated tooth restored with a post was predicted using the finite element method. The FE studies employed the software ANSYS (version 8) (5, 6) for its solid modeling (Figure 1).

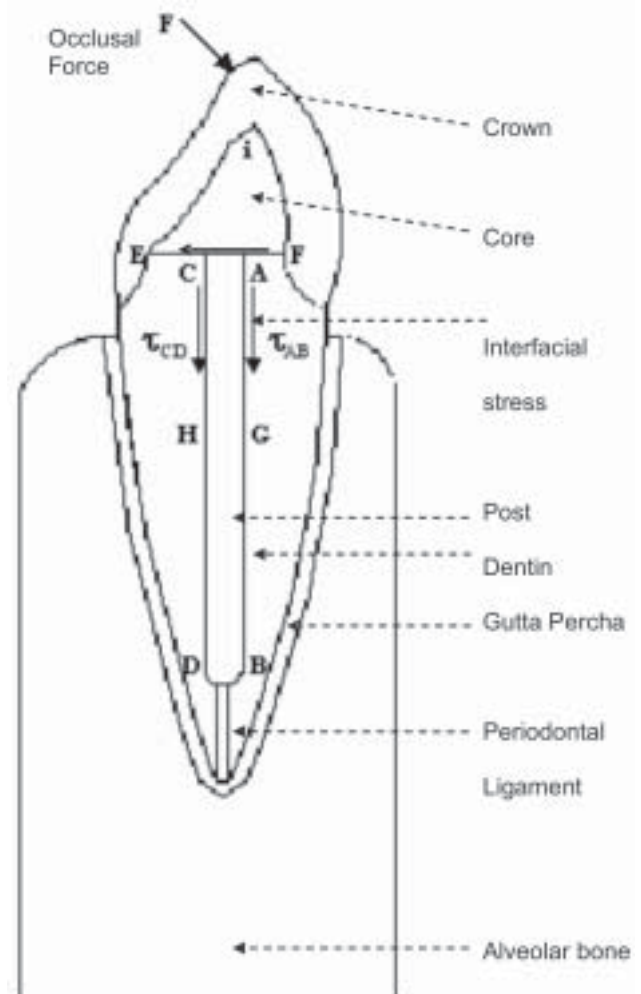


FIGURE 1 -2-D finite element solid model of the tooth specimen included the ligament and alveolar bone sections. A load of 250 N was introduced on the occlusal surface. The directions of interfacial stresses (t_{AB}) under occlusal loading

The two-dimensional FEM was created by a self-developed image processing system, manually digitizing the key points on dental cross-section boundaries obtained from an actual maxillary canine tooth image. Crown, post core and coronal-radicular restoration were modeled by creating key points and transferring them to a two-dimensional coordinate XY system in the FE environment. The generated post in the model was 1.4 mm in diameter and 15 mm in length.

The 2D FE analyses were employed because the studied geometry was complex and fine mesh generation was needed on the post dentin interface for accuracy on the interface shear stress results. Usually the three-dimensional FE models can capture the geometry of complex structures more fully than the two-dimensional FE models. However, the complexity of 3D FE models often makes it impossible to achieve the same mesh refinement and hence numerical accuracy as in 2D models.

Material properties

All the materials and vital tissues were presumed elastic, homogenous and isotropic, which included continual interfaces between materials. The structural properties of these materials were determined according to a literature survey (7, 8, 9). Table 1 reveals that each component of the tooth-restoration system was attributed to either the corresponding elasticity modulus value of the dental tissue or of the material that it represented.

TABLE 1 - Mechanical properties of materials included in the finite element model

Material ratio	Young's modulus (GPa)	Poisson's
Porcelain Jacket Crown	69	0.28
Composite Core	8.3	0.28
Post Material	200	0.33
Dentin	18.6	0.31
Gutta Percha	0.069	0.45
Periodontal Ligament	0.0689	0.45
Alveolar bone	13.7	0.30

Element description

For the FE analysis, the tooth structure was divided into 1919 elements of varying size, corresponding to 5890 nodal points (Figure 2).

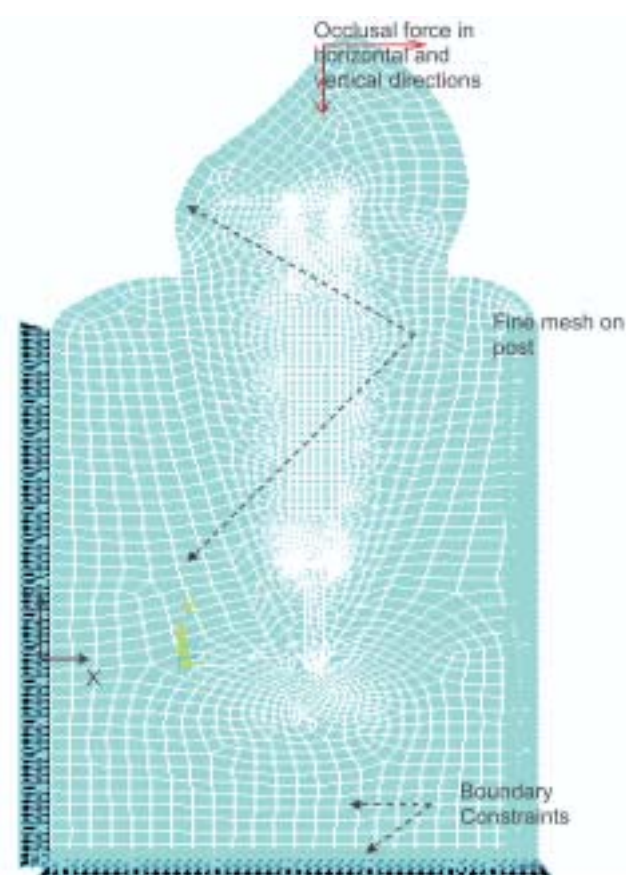


FIGURE 2 - Mesh, force, and boundary constraints in X-Y directions in the FE structure. Fine meshes on the post

Element PLANE82 was used in the FE modeling. These elements provide more accurate results for mixed (quadrilateral-triangular) automatic meshes, and can tolerate irregular shapes with little loss of accuracy. These types of elements have compatible displacement shapes and are well suited to model-curved boundaries. The element was defined by eight nodes, each node having two degrees of freedom.

There were two main reasons for using PLANE82 element in the FEM analysis. First, the element solution accuracy degrades as elements are distorted. This degradation is more pronounced for linear elements than it is for quadratic elements. The degradation in performance for linear elements is most pronounced for bending loads coupled with irregular element shapes. Second, the PLANE82 continuum element has an acceptable shape. The Jacobian ratio-shape parameter of PLANE82 is

within the acceptable element shape limits whose default values are functions of the element type and the settings.

The PLANE 82 quadratic element provided very good performance under the occlusal loading. This good performance was attributed to the ability of the PLANE 82 elements to properly handle bending, in contrast to the linear elements.

Mesh size and configuration

Mesh size and configuration were important aspects of finite element modeling. One of the main concerns in a finite element analysis was the adequacy of the finite element mesh. Precise mesh refinement was obtained in the bottom and top of the post regions where high stress intensity were expected. Mesh was chosen to be especially fine in this area, as well as along the post-dentin interface. Much effort and time was spent in the meshing procedure to avoid creating ill-conditioned elements. An error-estimation technique was utilized to calculate the amount of solution error due specifically to mesh discretization.

However, the ability to generalize these results is limited due to the assumptions that the tooth components can be modeled as homogeneous, isotropic, linear-elastic materials (plastic effects are ignored in this investigation), these results can be considered shortcomings of this study. Nevertheless, shortcomings of this study could be overcome by defining heterogeneous and anisotropic models for the tooth.

Loading

The two-dimensional tooth model was subjected to 50, 100 and 250 N (Newton) external occlusion chewing forces (10) on top of the crown shown in Figure 1 with F symbol, although lower biting forces were published (11). The loading direction was diagonal, with a 45-degree angle with respect to the implant axis (Figure 2). The exterior nodes on the surfaces of the alveolar bone were constrained (fixed) in all directions as the boundary conditions.

RESULTS AND DISCUSSION

External occlusal forces of 50, 100, and 250 Newton upon a tooth structure created normal and interfacial stresses that were very important variables for the assessment of post-dentin bonding strength. The interfacial stresses were calculated along the AB path as the average of the values belonging to two adjacent elements opposite to the bond interface. Interfacial stress (t_{xy}) results were virtually mapped onto AB path through the post. The computed interfacial stress (t_{xy}) results varying along the AB path are shown in Figure 3. in the form of a tabular listing under 250 occlusal force. Post lengths $x=0$ and $x=15$ mm marks the top and the bottom of the post, respectively. High changes in interfacial shear stress were observed for the range of occlusal loads that were considered. These variable stress patterns suggest that increasing the occlusal force would increase the interfacial shear stress between the post and the dentin.

Viewing Figure 3, it was observed that the occlusal force created a distinctive pattern of stresses.

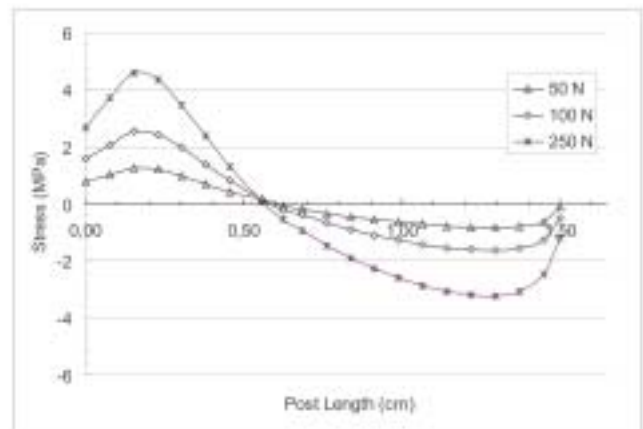


FIGURE 3 - Distribution of interfacial stress between post and dentine surface on the AB surface in 0.1 cm intervals. For 50, 100, and 250 loadings minimum interfacial stress were obtained approximately one third of the post length

The interfacial stresses along the post were roughly sinusoidal. Two sites of severe stress concentrations were identified. For example, under 250 Newton occlusal forces, the interface between the post and the dentin received peak interfacial stress values equal to 4.6 Mpa ($x=0$ mm) and -3.2

MPa ($x=14$ mm) in the positive and negative directions of Y axis, respectively. The interfacial stresses were virtually zero over one third of the post interface ($x=5$ mm). Similar trends were obtained under 50 and 100 Newton occlusal loadings.

A comparison with the results of 1.5 cm post applications indicated that the increasing load from 50 Newton to 100 Newton and from 100 Newton to 250 Newton increased the interfacial shear stresses approximately 36% and 45%, respectively.

As demonstrated by finite element stress analyses, the non-uniformity of the interfacial stress distribution indicates that fracture initiation may start from flaws at the interface at areas of high localized stress (12, 13). Interfacial stress concentration region lies on the top or close to bottom of the post. This indicates that the interfacial failure initiation should be expected to start from the top of the post.

The transition between positive and negative interfacial stresses occurred at point G that was located one third of the post; in fact, the value of interfacial stresses reached zero at point G. Increasing the occlusal force from 50 to 250 Newton did not change the transition point (Figure 3).

The magnitude of the vector forces at the top of the post were from left to right and were higher than the bottom. The vector arrows directions at bottom of the post were in the opposite direction of the loading force applied from right to left. Another finding was that force vectors magnitudes were almost zero at one third depth of the post length indicating no stresses. We can assume that the tooth is pinned and is expected to turn around at this point, even though, in reality there is no such thing. This means we could expect less interface shear stress around the post at this point.

Multiple regression analyses were used to discover the relationship between the independent (or predictor) variable post length and the dependent variable interfacial stress and then finding an equation that satisfies that relationship. All variables were entered into the regression equation according to the standard regression method. Linear, second order polynomial trend line and functional regression equations relating interfacial stress to post length under 50, 100, and 250 N occlusal forces were developed (Table 2).

TABLE 2 - Linear, second order polynomial trend line and functional regression equations

F= 250 N	F= 100 N	F = 50 N
Interfacial stress (MPa)	Interfacial stress (MPa)	Interfacial stress (MPa)
$t_{xy} = 3.7-5.25L$	$t_{xy} = 2.1-2.7L$	$t_{xy} = 1.1-1.4L$
$t_{xy} = 4.2L^2-11.62L+5.24$	$t_{xy} = 2.44L^2-6.42L+3$	$t_{xy} = 1.23L^2-3.2L+1.5$
$t_{xy} = 4\sin(4(L+0.25))+0.15$	$t_{xy} = 1.6\sin(3.1(L+2.5))+0.2$	$t_{xy} = 0.9\sin(3(L+0.5))+0.2$

Vector displays were used in the structural analysis to see how the tooth structure was deformed under the applied loads. Vector display of arrows showed the variation of both the magnitude and direction of a vector quantity in the tooth model (Figure 4).

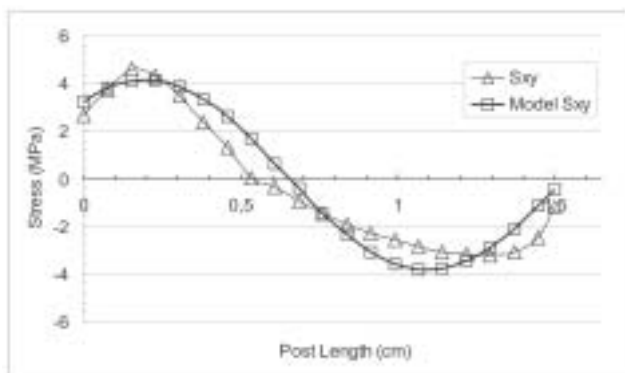


FIGURE 4 -Distribution of interfacial stress between post and dentine surface on the AB surface under 250 Newton occlusal force. From the plot, it looks like a sinusoidal model will fit the data well. The highest interfacial stress value was computed at the top of post

In all three models independent variables were significant ($p < 0.005$). R^2 values of the linear and the second order polynomial trend line three regression equations were 0.8.

Figure 3 demonstrates that the interfacial stress along the post was not linear but nonlinear. To include the interfacial stress nonlinearity, a

sinusoidal curve shown in Figure 4 was fit to the graph. The sinus function in this formula was converted to radians mode. This sinusoidal model was tested by graphing it on top of the interfacial stress data obtained by the FE analysis. The loading sites of forces and the mechanism of deformation of the tooth structure are shown in Figure 5.

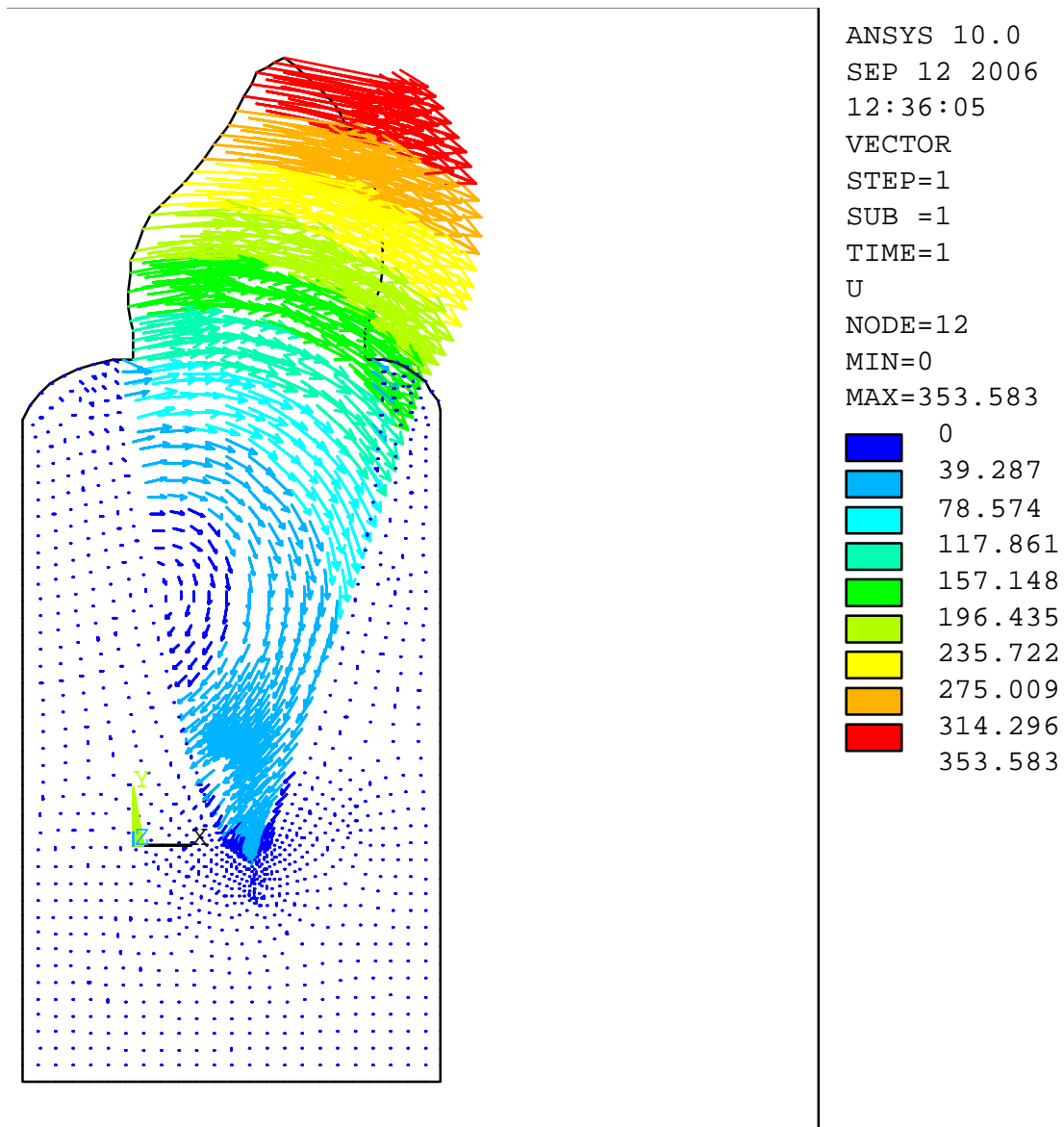


FIGURE 5 - Vector arrows indicate loading sites of forces and the mechanism of deformation of the tooth structure. The parameters MIN and MAX were used to specify the limits of the color intensity scale for the magnitude of the vector. The vector directions varied along the post indicating the rotation of the tooth under the loading force

Although the model was not the exact, most of the original points were hit. Therefore, we can say that the constitutive model for interfaces was able to capture the characteristic interfacial behavior of the post-dentin surface under the specific loading conditions under consideration. Thus, for any given force applied compressively at 45 degrees angle with respect to the implant axis, it is possible, by use of the described equation, to calculate the interfacial shear stress.

CONCLUSION

A finite element (FE) analysis was performed to investigate the interfacial shear stress distribution on the dentine-post interface frequently used for the restoration of endodontically treated dental elements. From the results and within the limitations of the present study it can be concluded that the interfacial stress along the post is nonlinear and is roughly sinusoidal and the peak interfacial stress between the post and the dentin is expected to occur on top of the post. Sinusoidal models were developed to generalize the interfacial stress nonlinearity along the post length. These models can be used for calculation of the interfacial shear stress for 50, 100, and 250 Newton forces applied compressively at 45 degrees angle with respect to the implant axis.

REFERENCES

1. Holmes DC, Diaz-Arnold AM, Leary JM. Influence of post dimension on stress distribution in dentin. *J Prosthet Dent.* 1996;75(2):140-7.
2. De Santis R, Prisco D, Apicella A, Ambrosio L, Rengo S, Nicolais L. Carbon fiber post adhesion to resin luting cement in the restoration of endodontically treated teeth. *J Mater Sci. Mater Med.* 2000;11(4):201-6.
3. Burns DA, Krause WR, Douglas HB, Burns DR. Stress distribution surrounding endodontic posts. *J Prosthet Dent.* 1991;66(1):141-2.
4. Alessandro L, Raffaella A, Sandro R, Davide A, Antonio A. 3D FEA of cemented steel, glass and carbon posts in a maxillary incisor. *Dent Mater.* 2005;21(8):709-15.
5. ANSYS user's manual. Chicago: Quintessence Publishing Co Inc; 1994.
6. ANSYS, Revision 8.0. Technical description of capabilities. Houston: Swanson Analysis Systems Inc; 1992.
7. Nakayama WT, Hall DR, Grenoble DE, Katz JL. Elastic properties of dental resin restorative materials. *J Dent Res.* 1974;53:1121-6.
8. De Santis R, Ambrosio L, Nicolais L. Mechanical properties of tooth structures. In: Ashman A, Bruin P. *Biomaterials in medicine and engineering.* New York: Plenum Publishing Co; 2002. p. 589-97.
9. Povo F, Hermida EB. Measurement of the elastic modulus of dental Pieces. *J Alloys Compounds.* 2000;310(1):392-5.
10. Gedrange T, Bourauel C, Kobel C, Harzer W. Three-dimensional analysis of endosseous palatal implants and bones after vertical, horizontal, and diagonal force application. *Eur J Orthod.* 2003;25(2):109-15.
11. Bosman F. Between biting and swallowing, physiology of mastication, *Ned Tijdschr Tandheelkd.* 1995;102(11):438-40.
12. Della Bona A, van Noort R. Shear versus tensile bond strength of resin composite bonded to ceramic. *J Dent Res.* 1995;74(9):1591-6.
13. Van Noort R, Cardew GE, Howard IC, Noroozi S. The effect of local interfacial geometry on the measurement of the tensile bond strength to dentin. *J Dent Res.* 1991;70(5):889-93.

Received: 03/01/2009

Recebido: 01/03/2009

Accepted: 03/30/2009

Aceito: 30/03/2009

Reviewed: 07/28/2009

Revisado: 28/07/2009